scientific reports

Check for updates

OPEN

Prostaglandin endoperoxide synthase 2 regulates neuroinflammation to mediate postoperative cognitive dysfunction in mice

Xuelian Li[1,2,3,5], Xuemei Li[1,3,5], Qixin Zhang[1,3], Yiyun Li[1,3], Yingshun Zhou[4]✉, Jun Zhou[1,3]✉ & Xiaoxia Duan[1,3]✉

Prostaglandin endoperoxide synthase 2 (PTGS2) is a rate-limiting enzyme of prostaglandin (PGs) production, mediating perioperative inflammatory response. This study aimed to explore the mechanisms underlying the involvement of PTGS2 in postoperative cognitive dysfunction (POCD). Transient bilateral common carotid artery occlusion (tBCCAO) was performed to induce POCD. The Morris water maze test was used to assess the cognitive function. PTGS2 expression in the hippocampus and plasma was measured. Hippocampal RNA sequencing was performed to determine the pathological basis of POCD. In vivo, the mice were treated with or without a selective PTGS2 inhibitor during the perioperative period. The hippocampi were isolated to detect inflammation and oxidative damage. In vitro, PTGS2 was silenced in BV2 microglial cell lines, and oxygen-glucose deprivation/reoxidation (OGD/R) was performed. Conditioned medium from BV2 cells was collected to culture HT22 hippocampal neurons. Proinflammatory factors and oxidative damage were detected in BV2 and HT22 cells, respectively. The results indicated that the expression of PTGS2 in the plasma and hippocampal tissue of POCD mice was increased and that hippocampal inflammation is an important biological process in POCD. Inhibition of PTGS2 alleviated hippocampal inflammation, and the Morris water maze test showed improved learning and memory functions that were previously impaired. In addition, the inhibition of PTGS2 prevents OGD/R-induced microglial activation and alleviates neuronal injury. In conclusion, PTGS2 may be a culprit in POCD.

Keywords Microglia, Neuroinflammation, Oxidative damage, Postoperative cognitive dysfunction, Prostaglandin endoperoxide synthase 2

Postoperative cognitive dysfunction (POCD) is a common perioperative neurocognitive complication observed in patients of all ages[1,2]. The combined incidence was approximately 29%, owing to the heterogeneity of the evaluation index and study participants[3]. POCD prolongs the hospital stay, induces depressive mood, and increases the risk of postoperative mortality[4]. Hence, understanding the mechanism of POCD can help establish preventive and control measures.

Growing evidence suggests that neuroinflammation is a potential contributor to POCD[5], leading to cognitive impairment through mechanisms such as increasing blood–brain barrier permeability and inducing mitochondrial dysregulation[6,7]. The inhibition of hyperactive neuroinflammatory responses is a common therapeutic strategy for POCD[8]. Microglia are major players in POCD-associated neuroinflammation[9]. Activated microglia have been frequently reported to upregulate the expression of Prostaglandin endoperoxide synthase

[1]Department of Anesthesiology, The Affiliated Hospital, Southwest Medical University, Luzhou 646000, Sichuan Province, China. [2]Department of Anesthesiology, First People's Hospital, Zigong 643000, Sichuan Province, China. [3]Anesthesiology and Critical Care Medicine Key Laboratory of Luzhou, Southwest Medical University, Luzhou 646000, Sichuan Province, China. [4]Department of Pathogen Biology, The Public Platform of the Pathogen Biology Technology, School of Basic Medicine, Southwest Medical University, Luzhou 646000, Sichuan Province, China. [5]Xuelian Li and Xuemei Li contributed equally as co-first authors. ✉email: yingshunzhou@swmu.edu.cn; junzhou@swmu.edu.cn; duanxiaoxia@swmu.edu.cn

2 (PTGS2)[10]. PTGS2 plays a pivotal role in inflammatory signaling and associated pathological processes. Under normal physiological conditions, PTGS2 expression is relatively low; however, it is rapidly upregulated in response to inflammatory stimuli or trauma[11]. As a key enzyme, PTGS2 catalyzes the conversion of arachidonic acid into prostaglandins, including PGE2, which act as critical mediators of inflammation[12]. PTGS2 not only modulates inflammatory responses by regulating signaling pathways such as nuclear factor-kappa B (NF-κB)[13], but also indirectly influences the expression of multiple proinflammatory cytokines, including interleukin-6 (IL-6) and tumour necrosis factor-alpha (TNF-α), through the production of PGE2[14].

In clinical practice, selective PTGS inhibitors have been shown to protect against postoperative cognitive decline. According to a retrospective population-based cohort study, the use of selective PTGS2 inhibitors reduced the risk of postoperative cognitive impairment by more than 15%[15]. Recent findings indicate that in adults with hyperlipidaemia who received parecoxib before surgery, the incidence of postoperative delirium was 13.72% and 12.39% lower than that in the placebo group[16]. Studies in animal models have shown that PTGS2 expression increases in the hippocampus after surgery[17,18]. Inhibiting hippocampal PTGS2 overexpression improves cognitive function in POCD rats[19].

In this study, we explored the possible mechanisms by which PTGS2 is involved in POCD.

Methods

Animals

Four-month-old male C57BL/6 mice weighing 26–30 g were used in this study (Chengdu Dossy Experimental Animals Co., LTD, China). In vivo experiments have been ethically approved by the Ethics Committee of Laboratory Animal Care and Welfare of Southwest Medical University, Chairman Minhai Nie, April 18, 2022 (approval number SWMU20220029, Luzhou, China). In addition, the experiments conformed to ARRIVE Guidelines 2.0 and were in accordance with the National Research Council's Guide for the Care and Use of Laboratory Animals. All the animals were housed in specialised rodent cages (n = 5/cage). Animals had ad libitum access to standard rodent chow and water under standard breeding conditions at 22 °C. Before the experiment, the animals were acclimated to natural light for one week.

Transient bilateral common carotid artery occlusion (tBCCAO) has been used to induce cognitive impairment in mice[20] to simulate POCD caused by intraoperative hemodynamic fluctuations[21]. In the first in vivo experiment, 28 mice were randomly assigned to the following two groups using simple randomisation (n = 14/group): control group and surgery group. Mice in the Surgery group underwent tBCCAO. Anaesthesia was administered with isoflurane, 4% for induction, and 2% for maintenance[22]. After 30 min, the mice with no response to pain were placed in the supine position and immobilised. In the middle of the neck, an incision (2 cm) was made. The bilateral common carotid arteries were separated, clamped for 10 min, and then reperfused for 10 min; this process was repeated three times. The incision was rinsed with saline and closed using sterile 4 – 0 surgical suture. The time from anaesthesia induction to resuscitation lasted for approximately 2 h. Postoperative analgesia was administered by intraperitoneal injection of fentanyl (2 μg/kg) and local infiltration of the incision with 2 mL of 1% ropivacaine. The mice in the control group underwent the same surgical procedure without ligation of the bilateral carotid arteries. The timeline shown in Fig. 1A illustrates the experimental protocol.

Eighty mice were randomly assigned to four groups (n = 20 mice/group): control, Cele, Sur, and Cele + Sur. According to a preclinical study[23], mice in the Cele and Cele + Sur groups received daily intraperitoneal injections of celecoxib (20 mg/kg/day; #DL2227, Pfizer Inc., United States) from 3 days preoperatively to 3 days postoperatively. In addition, mice in the control and Sur groups received intraperitoneal injections of the same volume of vehicle (normal saline containing 20% dimethyl sulfoxide [; #D8370, Solarbio, China]). The mice in the Sur and Cele + Sur groups underwent tBCCAO. The timeline shown in Fig. 2A illustrates the experimental protocol.

Cell treatment

The BV2 mouse microglial cell line (RRID: CVCL_0182) and HT22 mouse hippocampal neuronal cell line (RRID: CVCL_0321) were used (Procell Life & Technology Co., Ltd., China). BV2 and HT22 cells were cultured with Dulbecco's Modified Eagle Medium (DMEM, #C11995500BT, ThermoFisher Scientific, United States) supplemented with 100 U/mL penicillin/streptomycin and 10% foetal bovine serum (#PS-FB5-SA1, PeakSerum, United States) in a carbon dioxide (CO_2) incubator (37 °C, 5%).

According to the manufacturer's protocol, short hairpin ribonucleic acid (shRNA) was transfected into BV2 cells (Hanbio Biotechnology Co., Ltd., China). The shRNA sequences are listed in Supplementary Table 1. shRNA-PTGS2 with a PTGS2 inhibition rate of 64.96 ± 3.01% (P < 0.0001) was selected for subsequent experiments (Supplementary Fig. 1 A-B).

BV2 cells were transfected with either shRNA-PTGS2 (B-sh-PTGS2 group) or shRNA-NC (negative control (B-NC group). These two groups were treated with oxygen-glucose deprivation/reoxidation (OGD/R), similar to the B-sh-PTGS2-OGD and B-NC-OGD groups. The conditioned media of BV2 cells in each group were collected and used for the corresponding HT22 cell culture[24].

In vitro POCD model: oxygen-glucose deprivation/reoxygenation (OGD/R)

According to a previous study[25], BV2 cells were maintained in glucose-free DMEM (#L160 KJ; Basal Media, China). Next, BV2 cells subjected to glucose deprivation were cultured in an oxygen-free environment in an AnaeroPack rectangular jar (#C-01; Mitsubishi Gas Company, Japan). After oxygen-glucose deprivation for 4 h, the BV2 cells were cultured DMEM containing 100 U/mL penicillin/streptomycin and 10% foetal bovine serum in a CO_2 incubator (37 °C, 5%) for 20 h.

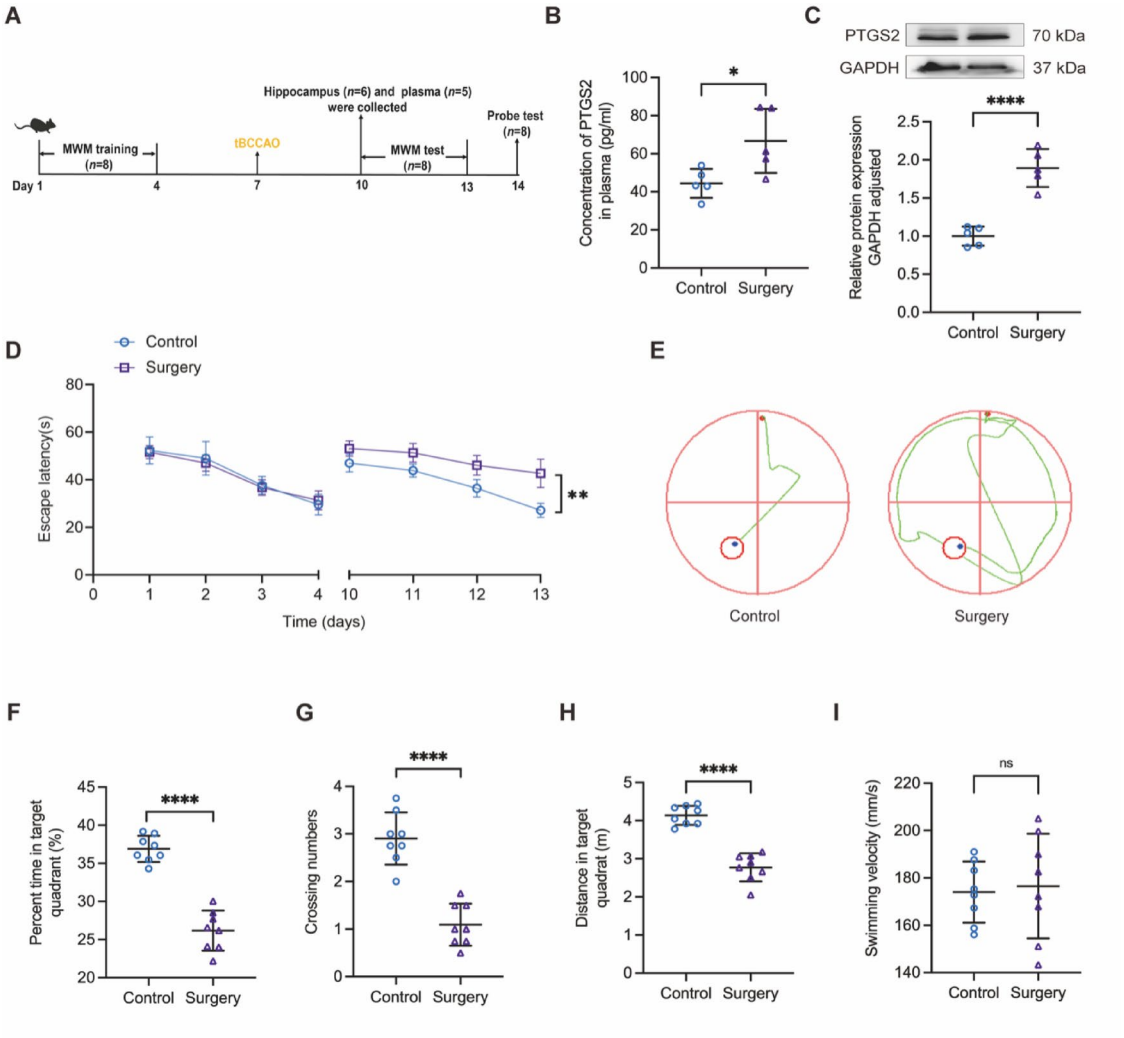

Fig. 1. Expression of PTGS2 in Plasma and Hippocampus were increased in POCD mice.

Enzyme-linked immunosorbent assay (ELISA)

On the 3rd postoperative day, mice were anaesthetised with 2% isoflurane. Blood was collected via enucleation of the eyeballs. The blood was mixed with heparin for 10 min and the supernatant (plasma) was collected by centrifugation (2000 g, 4℃, 20 min). The plasma PTGS2 concentration was detected using the Mouse PTGS2/COX-2 ELISA Kit (#AD2829Mo; Andy Gene Biotechnology Co., Ltd., United States).

Brain tissue collection

Three days after surgery, the mice were deeply anaesthetised with isoflurane. Cardiac perfusion was performed using pre-cooled 0.9% normal saline (10% neutral formaldehyde for haematoxylin and eosin [H&E] staining and immunohistochemical analysis). The mice were then decapitated by trained experimenters[26] Hippocampi were isolated on ice and stored at −80℃ for subsequent experimental analysis.

RNA-seq

Total RNA was extracted from the hippocampi of the control and Sur groups (n = 6/group) was extracted using TRNzol Universal Reagent (#DP424, TIANGEN, China). Sequencing was performed using the Illumina NovaSeq 6000, and raw data were saved as FASTQ files. After quality control, differentially expressed genes (DEGs) were identified (edgeR, v3.24.3). Blast2 go (v2.5) and KOBAS (v2.0) were used to annotate gene ontology (GO) functions and the Kyoto Encyclopedia of Genes and Genomes (KEGG) pathways[27–29], respectively. The STRING database (v11.5) was used for protein interaction analysis and the results were visualised using Cytoscape (v3.6.1).

Morris water maze (MWM)

According to the MWM protocol, cognitive function was assessed[30]. MWM was performed in a 122 cm diameter circular pool, evenly divided into four quadrants. White coloured water at 25℃ was added to a depth of 35 cm. A hidden platform was placed 1 cm below the water surface. MWM training was initiated 7 days preoperatively

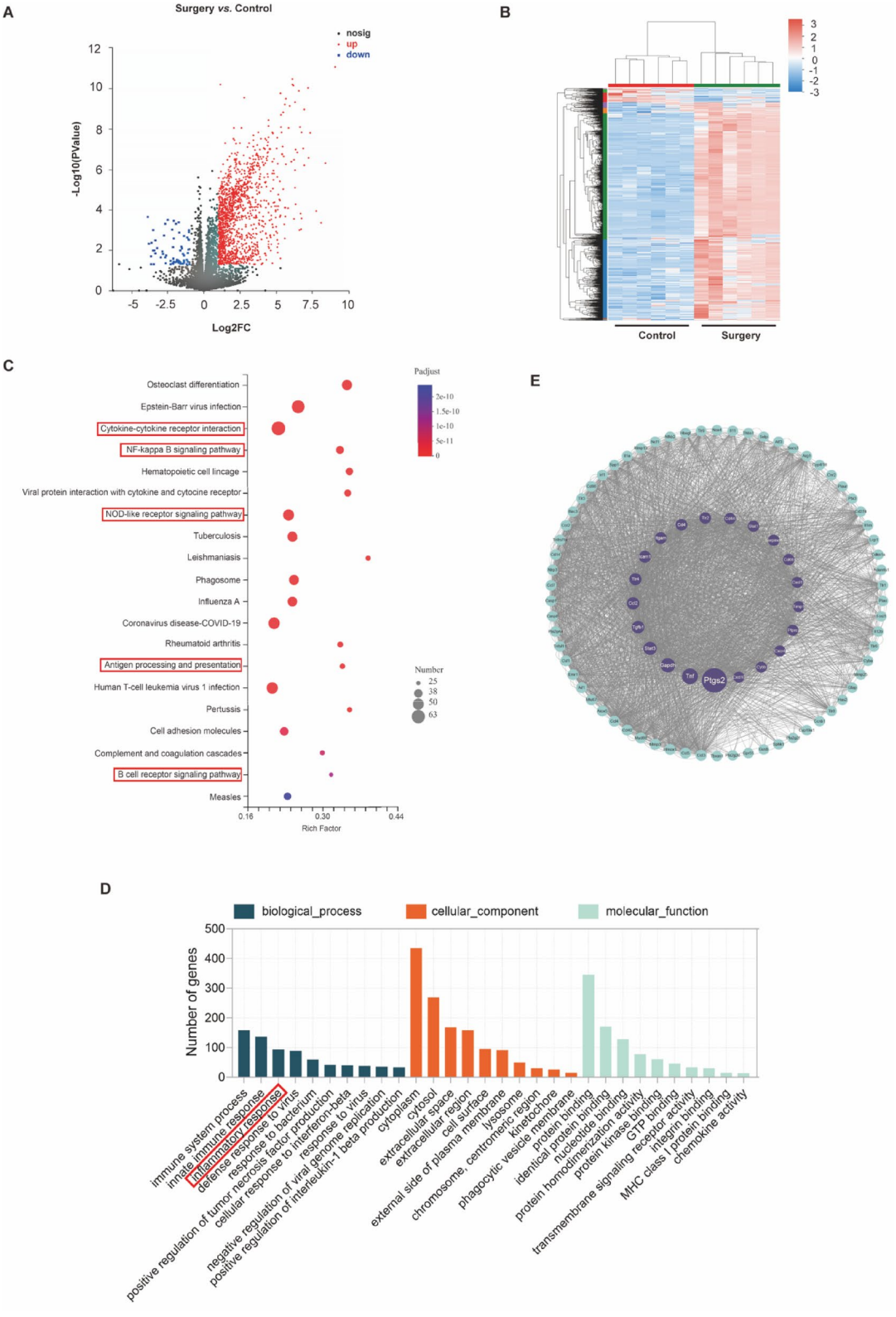

Fig. 2. PTGS2 contributes to the development of POCD.

and continued for four consecutive days. From the third postoperative day, each mouse was tested four times a day at 3-min intervals for 4 days. Twenty-four hours after the last day of spatial acquisition, a probe test was conducted. During spatial acquisition, the mice were placed in the pool with the nose tip facing the wall, and the time taken to reach the platform was recorded. If a mouse failed to find the platform within the specified time (60 s), it was manually guided to the platform and the recording time was set to 60 s. The mice were then left on the

platform for 15 s. After 3 min, the mice were placed in the pool again, starting from an adjacent quadrant relative to the previous experiment, ensuring all four quadrants were tested in clockwise manner. During the probe test, the hidden platform was removed, and the mice were placed in the swimming pool allowed to swim from the same position for 60 s. The percentage of time spent in the target quadrant, number of times the platform was crossed, swimming distance, and swimming speed within the target quadrant were recorded and analysed. All swimming activity was tracked and analysed using the WMT-100 Morris software (Taimeng Software Co., Ltd., China).

H&E staining

Based on a previous study, 4-μm paraffin sections were prepared[31] Then, the sections were scanned using an automatic digital pathological section scanner (#KF-TB-400, Konfoong Biotech International Co., LTD, China).

Immunohistochemistry

Paraffin sections of the mouse brain (4-μm) were dewaxed and the antigen was repaired. The sections were then blocked in bovine serum albumin and incubated with a primary antibody (ionised calcium-binding adapter molecule 1, Iba-1, #DF6442; Affinity Biosciences, United States). After washing with PBS, the cells were incubated with a secondary antibody (#S0001; Affinity Biosciences, United States). Wash again with PBS, it was stained with 3,3'-diaminobenzidine (#DA1010, Solarbio, China) and haematoxylin, dehydrated with ethanol, rendered transparent with xylene, and finally sealed with neutral gum. The antibodies used in this study are listed in Supplementary Table 2.

Quantitative real-time polymerase chain reaction (qRT-PCR)

Total RNA was extracted using TRNzol Universal Reagent (#DP424, TIANGEN, China). The concentration and OD260/280 were determined using a NanoDrop spectrophotometre (Thermo Fisher Scientific Inc., United States). The RNA was reverse-transcribed into copied DNA (#FSQ-301; TOYOBO, Japan). qRT-PCR analysis was performed with SYBR Green fluorescent dye (#QPK-201, TOYOBO, Japa) on a Roche PCR instrument (LightCycler®96, F. Hoffmann-La Roche, Ltd, Switzerland). The primer sequences used are listed in Supplementary Table 3.

Western blotting

Total protein in the hippocampi and cells was extracted using RIPA lysis buffer (#P0013B, Beyotime, China) containing 1% PMSF (#P0100, Solarbio, China). Proteins were separated by 12% SDS-PAGE and transferred to a PVDF membrane (#IPVH00010, Millipore, Germany). The membrane was blocked with 5% skim milk and washed with Tris-buffered Saline containing Tween-20. Western Blotting analysis was performed using primary antibodies (Iba-1, #DF6442, RRID: AB_2838405, Affinity Biosciences, United States; Cox2, # AF7003, RRID: AB_2835311, Affinity Biosciences, United States; Ferritin Heavy Chain [FTH1], # DF6278, RRID: AB_2838244, Affinity Biosciences, United States; divalent metal transporter 1 [DMT1], # DF12740, RRID: AB_2845701, United States; glutathione peroxidase 4 [GPX4], # DF6701, RRID: AB_2838663, United States) and secondary antibody (#S0001, RRID: AB_2839429, Affinity Biosciences, United States) (Supplementary Table 2). The immunoreactive bands were visualised using a gel imager (GelView 5000Plus Smart Gel Imaging System; Guangzhou Biolight Biotechnology Co., Ltd., China). ImageJ software (National Institutes of Health, Bethesda, MD, USA) was used for quantitative analysis.

Malondialdehyde (MDA) detection

MDA can be condensed using thiobarbituric acid, and the product exhibits a maximum absorption peak at 532 nm. According to the manufacturer's instructions, 5 mg of fresh hippocampus was homogenized and treated, the MDA concentrations were quantified using an MDA assay kit (#A003, Nanjing Jiancheng Bioengineering Institute, Nanjing, China) according to the manufacturer's instructions.

MTT assay

The MTT assay was used to evaluate the viability of HT22 cells. HT22 cells were seeded into 96-well plates (5×10^3 cells/well). After 20 h of treatment with the conditioned medium, MTT (5 mg/mL/well, #M8180, Solarbio, China) was added and incubated at 37 °C for 4 h. The formazan crystals were dissolved in DMSO (150 μL/well). The absorbance (570 nm) was measured (BioTek, Santa Clara, United States).

Reactive oxygen species (ROS) measurement

Intracellular ROS levels were detected using a Reactive Oxygen Species assay kit (#CA1410; Solarbio, China). HT22 cells were cultured in 6-well plates (5×10^5 cells/well). After treatment with the conditioned medium for 24 h, washed cells with serum-free medium and stained with 7 μM 2′,7′-dichlorofluorescin diacetate (DCFH-DA) for 40 min. Subsequently, the cells were washed thrice with serum-free medium. Images were captured using an inverted fluorescence microscope (#IX73, OLYMPUS Corporation, Tokyo, Japan) with an FITC channel (excitation wavelength: 488 nm, emission wavelength: 525 nm).

Statistical analysis

Statistical analyses were performed using GraphPad Prism 9.0.0 (San Diego, CA, USA). The sample size depended on the POCD modelling method used in the study[20,32] The researcher was blinded to the experiment and data analysis. No exclusion criteria were set and no animals considered for the experiment were excluded. No animals died during the experiment. No outlier tests were performed on the data. A normality test was conducted on the data, and data conforming to a normal distribution were expressed as mean ± standard deviation. A two-

tailed Student's t-test was used to compare two groups. Welch's t-test was used when the two groups of data had inconsistent variance. Differences between more than two groups were assessed using one-way analysis of variance (ANOVA). The escape latency in the Morris water maze was analysed using two-way repeated measures ANOVA. In the RNA-seq analysis, the probability or frequency of errors in the overall inference results was controlled by performing false discovery rate correction using the Benjamini/Hochberg algorithm to correct the *P*-value obtained from the statistical test. The corrected *P*-value was marked as P-adjusted. Significant differences are indicated by $^{*}P < 0.05$, $^{**}P < 0.01$, $^{***}P < 0.001$, $^{****}P < 0.0001$, and ns (non-significant differences).

Results

Expression of PTGS2 in plasma and hippocampus were increased in POCD mice

Expression of PTGS2 in plasma (66.73 ± 16.84 pg/mL in the Surgery group vs. 44.40 ± 7.58 pg/mL in the Control group; $P = 0.027$; Fig. 1B) and hippocampus ($P < 0.0001$; Fig. 1C) were increased 3 days after tBCCAO. In the MWM test, mice that underwent tBCCAO spent more time finding the target platform ($F_{(3,42)} = 4.593$, $P = 0.0072$; Fig. 1D-E). In the probe trial, the percentage of time spent in the target quadrant ($P < 0.0001$), number of crossings ($P < 0.0001$), and distance travelled in the target quadrant were reduced ($P < 0.0001$; Fig. 1F-I). These results indicated that tBCCAO induces cognitive decline.

PTGS2 May affect POCD-related inflammatory responses

Hippocampal RNA-seq showed that 1444 genes were significantly altered in mice, of which 1374 were upregulated and 70 were downregulated (surgery group vs. control group, Fig. 3A and B; top 100 DEGs are shown in Supplementary Table 4). KEGG pathway analysis showed that immune- and inflammation-related signalling pathways were highly enriched: the cytokine-cytokine receptor interaction, chemokine signalling pathway, NF-kappa B signalling pathway, NOD-like receptor signalling pathway, antigen processing and presentation, and B cell receptor signalling pathway (Fig. 3C). GO enrichment analysis of these DEGs revealed that the inflammatory response ranked third among biological processes (Fig. 3D). PTGS2 in the peripheral circulation can enter the centre through the blood-brain barrier[33]. Protein-Protein Interaction Networks (PPI) analysis of these DEGs revealed that 84 genes were closely associated with PTGS2 expression (Fig. 3E, Supplementary Table 5). These genes were mainly concentrated in the pathways identified in the KEGG analysis (Supplementary Table 6). These results support the role of neuroinflammation in POCD and indicate that the regulation of PTGS2 may affect POCD-related inflammatory responses.

PTGS2 contributes to the development of POCD

Western Blotting showed that celecoxib administration prevented the increased expression of PTGS2 induced by intraoperative cerebral ischaemia–reperfusion injury (CIRI) ($P = 0.0004$, $t[6] = 7.246$; Fig. 2B). According to the MWM test, celecoxib treatment did not affect the latency to locate the target platform ($F_{(3,54)} = 0.04492$, $P = 0.9872$; Fig. 2C-D). However, pharmacological inhibition of PTGS2 improved intraoperative CIRI-induced cognitive decline, and escape latency was significantly shortened by 26.9% ($F_{(3,54)} = 3.408$, $P = 0.0239$; Fig. 2C-D). Furthermore, the percentage of time spent in the target quadrant, number of crossings in the platform quadrant, and distance travelled in the target quadrant in the probe test increased by 38.8% ($P < 0.0001$), 93.6% ($P < 0.0001$), and 39.8% ($P < 0.0001$), respectively (Fig. 2E-G). In addition, there were no significant differences in swimming velocity ($F_{(3,36)} = 0.6414$, $P = 0.5934$; Fig. 2H).

PTGS2 mediation of hippocampal microglia activation and oxidative damage in the development of POCD

Immunohistochemistry revealed that pharmacological inhibition of PTGS2 decreased the percentage of Iba-1-positive areas in the hippocampus induced by CIRI ($P < 0.001$; Fig. 4A-B). This was supported by western blot analysis, which showed that inhibition of PTGS2 reduced hippocampal Iba-1 protein expression ($P = 0.0238$; Fig. 4C). qRT-PCR analysis showed that inhibiting PTGS2 exhibited suppression effects on POCD associated inflammation in the hippocampus: the activated microglia markers cluster of differentiation 68 (CD68) ($P = 0.0001$), TNF-α ($P = 0.0012$), IL-6 ($P = 0.0381$), and interleukin-1 (IL-1β) ($P = 0.0072$) were decreased significantly (Fig. 4D). H&E staining of the hippocampi showed that neurones in the surgery group were irregularly shaped, with darkly stained nuclei and chromatin condensation. Pharmacological inhibition of PTGS2 improved the damage to hippocampal neuron morphology after surgery (Fig. 5A) and reduced the production of MDA (a product of lipid peroxidation) in the hippocampus postoperatively ($P = 0.0088$; Fig. 5B). Furthermore, the inhibition of PTGS2 prevented the increased expression of FTH1 ($P = 0.0026$), DMT1 ($P = 0.0289$), and GPX4 ($P = 0.0155$) induced by intraoperative CIRI (Fig. 5C-D).

PTGS2 are required for OGD/R-induced microglial activation

We established an in vitro model of POCD to verify the involvement of PTGS2 in the regulation of microglial activation (Fig. 6A). PTGS2 expression was successfully inhibited in BV2 microglia, as evidenced by a decrease in protein and RNA levels of 35.1% ($P = 0.0015$) and 58.7% ($P = 0.0025$; Fig. 6B-D), respectively. Furthermore, PTGS2 inhibition prevented the upregulation of the microglial marker Iba-1 ($P = 0.0013$; Fig. 6B-C), decreased the expression of TNF-α ($P = 0.0134$), IL-1β ($P = 0.0037$), IL-6 ($P = 0.0273$), and CD68 ($P = 0.0008$) in BV2 cells induced by OGD/R (Fig. 6D).

PTGS2 mediates OGD/R-induced microglia neurotoxicity

The BV2 microglia-conditioned medium was collected from HT22 hippocampal neuron cultures (Fig. 7A). Downregulation of PTGS2 in BV2 microglia protected HT22 cells from damage caused by conditioned medium derived from OGD/R-induced BV2 microglia, prevented the decline in HT22 cell viability ($P = 0.0039$; Fig. 7B),

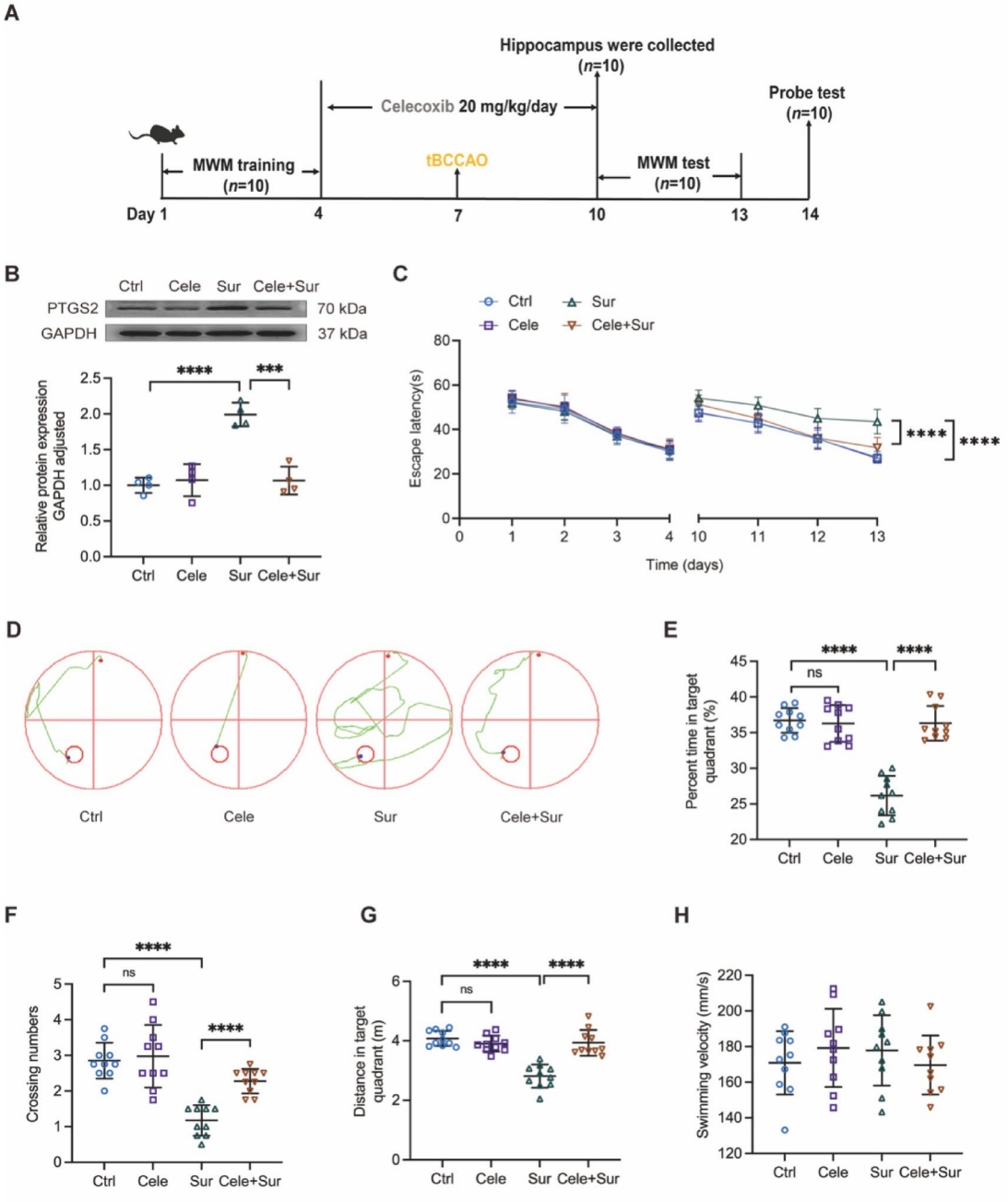

Fig. 3. Involvement of neuroinflammation in POCD development and association of PTGS2 with POCD-related microglial activation.

reduced intracellular ROS accumulation ($P < 0.0001$; Fig. 7C-D), inhibited the increase in DMT1 ($P = 0.0300$) and FTH1 ($P = 0.0291$), and restored the expression of GPX4 ($P = 0.0107$; Fig. 7E-F).

Discussion

Postoperative cognitive dysfunction (POCD) is classified as perioperative neurocognitive disorders (PND)[34], is of concern because it increases the risk of long-term cognitive decline such as dementia in the future[35]. Elderly patients who do not have a diagnosis of mild cognitive impairment or dementia but experience postoperative delirium or cognitive dysfunction, are three times more likely to develop permanent cognitive impairment or dementia[36]. The present study demonstrates that PTGS2 is involved in the development of POCD and that the underlying mechanism involves the regulation of microglia-mediated neuroinflammation.

The key pathogenesis of POCD is cerebral ischaemia–reperfusion injury (CIRI)-associated neuroinflammation[37,38]. Cerebrovascular disease, also known as cerebrovascular accident or stroke, may reduce patient tolerance to anaesthesia and increase the risk of perioperative neurocognitive disorders[39]. In

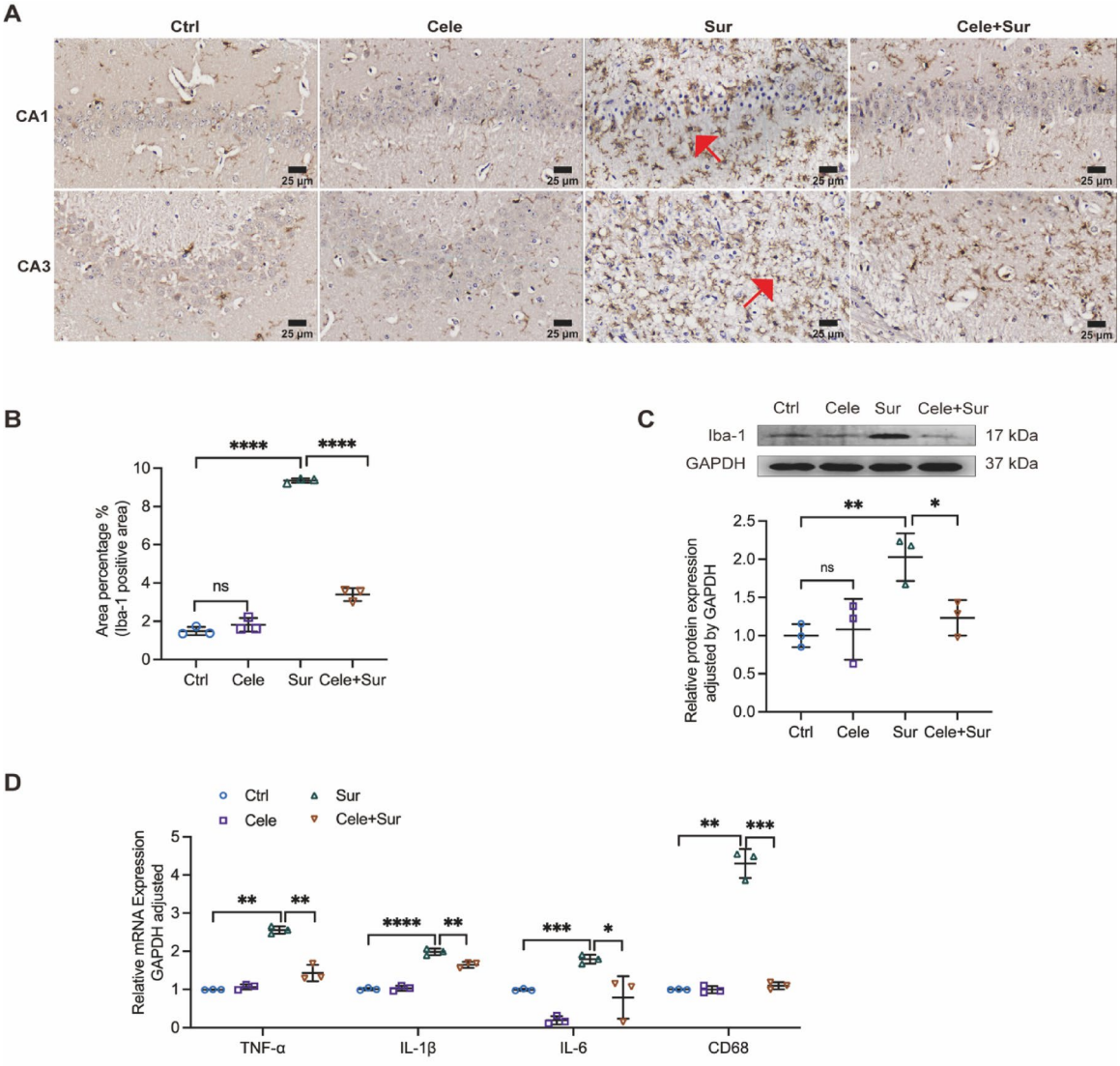

Fig. 4. PTGS2 mediation of hippocampal microglia activation in the development of POCD.

addition to existing cerebrovascular diseases, perioperative anaesthesia and surgical stress can induce acute cerebral ischaemia, also known as perioperative covert stroke. The incidence of cognitive decline one year after perioperative covert stroke was higher than that in non-stroke patients (42% vs. 29%)[40]. We established a POCD model by inducing CIRI in mice. We evaluated the cognitive function of the mice using the Morris water maze test to confirm that BCCAO treatment successfully induced POCD.

According to a previous study, following total hip replacement, patients with POCD have substantially greater levels of PTGS2 expression in their peripheral blood than those without POCD[41]. We revealed that mice with POCD have higher PTGS2 concentration in their peripheral blood. The maintenance of normal cognitive function is highly dependent on the hippocampus of the brain[42,43]. In this study, hippocampal PTGS2 expression was elevated in mice with POCD. It has been hypothesised that PTGS2 plays a role in POCD.

According to hippocampal RNA-seq studies, hippocampal inflammation may play a significant biological role in the onset of POCD. Research has verified the ability of specific PTGS2 inhibitors, including celecoxib, to cross the blood–including celecoxib[44]. Parecoxib, a selective inhibitor of PTGS2, suppressed IL-1β and TNF-α expression in the hippocampus after hepatectomy by down-regulating the PTGS2/PGE2 pathway[45]. In this study, specific PTGS2 inhibitor pretreatment can diminish the expression of inflammatory factors TNF-α, IL-1β and IL-6 in hippocampus of POCD model mice.

Microglia are the main innate immune cells involved in neuroinflammatory responses and are closely associated with the normal maintenance of synaptic plasticity and neuronal function[46,47]. Eliminating microglia can prevent synaptic loss and improve cognitive impairment induced by sevoflurane anesthesia[48]. Throughout the various stages of microglia activation, CD68 is broadly expressed. Because CD68 is mostly expressed in intracellular lysosomes, it is not a good tool for examining microglia morphology[49]. Iba-1 immunostaining can be used to assess the pathophysiological involvement of activated microglia in ischemia injury since[50]. This study

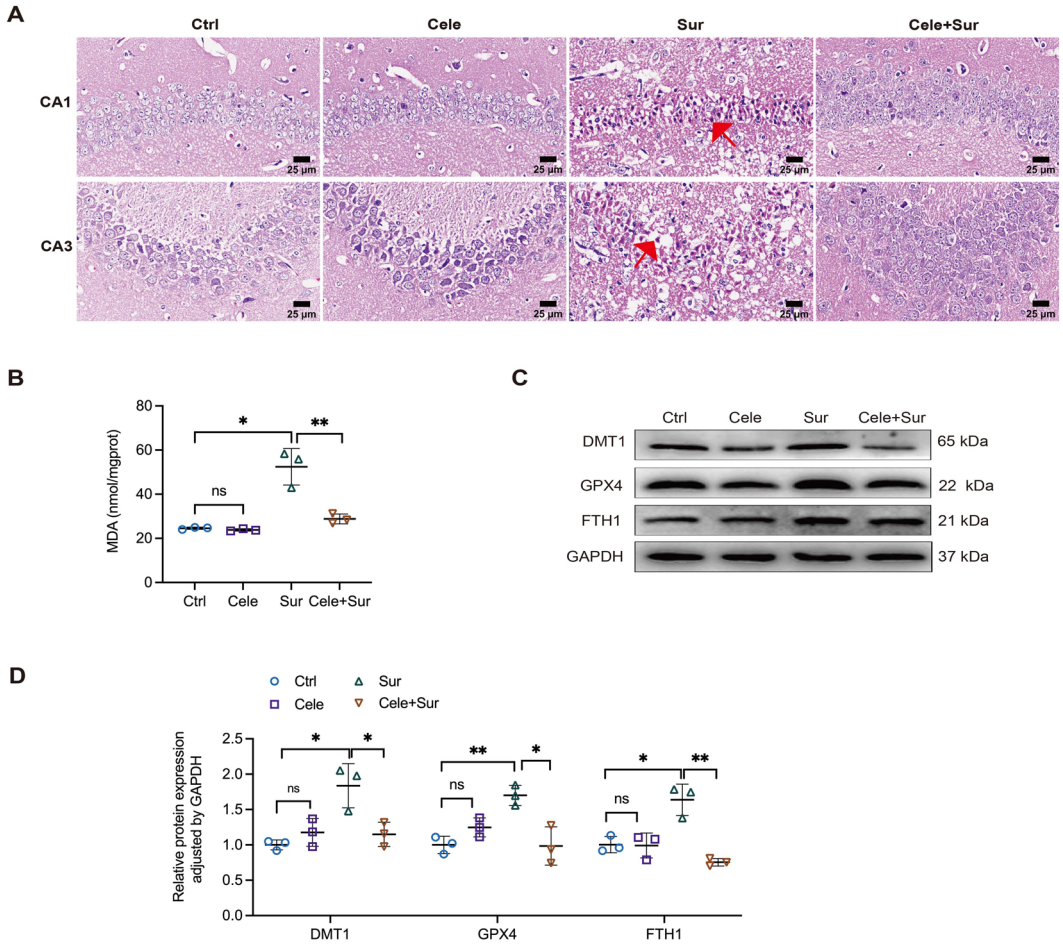

Fig. 5. PTGS2 mediation of hippocampal oxidative damage in the development of POCD.

indicated that preconditioning with specific PTGS2 inhibitors can reduce the expression of Iba-1 and CD68 in the hippocampus of POCD mice, suggesting that PTGS2 is involved in the regulation of microglial activation.

Microglia are the main source of PTGS2 in the central nervous after cerebral ischemia[51,52]. In a splenectomy mouse model, an intraperitoneal injection of the selective PTGS2 inhibitor meloxicam was administrated 24 h after surgery, reduced postoperative hippocampal microglial activation[53]. Compared with previous studies on the relationship between PTGS2 and POCD, we designed an in vitro study to explore the role of microglial PTGS2 in POCD-associated neuroinflammation. Changes in microglia during cerebral ischaemia-reperfusion were simulated by inducing oxygen glucose deprivation followed by reoxygenation (OGD/R)[54]. Here, we found that OGD/R induced an increase in PTGS2 expression in microglia, accompanied by an increase in inflammatory cytokines. The conditioned medium produced by the OGD/R treatment of microglia increased the levels of the iron storage proteins FTH1 (an iron-storage protein) and DMT1 (a major iron transporter) in neurones, while lowering neuronal activity, which is consistent with previous research. Inflammatory activation of microglia induces the internalisation of iron-exporting proteins in co-cultured neurones[55], significantly upregulating the expression of FTH1 and DMT1, and leading to iron accumulation in neurones[56]. Intracellular iron accumulation disrupts REDOX homeostasis and catalyzes reactive oxygen species (ROS) production, leading to oxidative damage[57]. Conditioned medium derived from OGD/R-induced microglia decreased GPX4 (intracellular antioxidant enzyme) levels in neurones, accompanied by an increase in neuronal ROS, which was alleviated after inhibiting PTGS2 expression in BV2 microglia. In conclusion, our results suggest that PTGS2 mediates the regulatory role of microglia in neuronal damage in an inflammatory setting, which requires confirmation in vivo. A recent study has shown that microglial activation induced by anaesthetics mediates excessive synaptic pruning and dendritic structural abnormalities[58]. Understanding how to assess and regulate microglia-neuron interactions, which are critical to brain health, will be key to developing effective treatments for POCD.

Studies have shown that the complete knockout of PTGS2 in rodents results in abnormal kidney development, reproductive abnormalities in females, patent ductus arteriosus, and spontaneous heart failure[59,60]. One day after the lateral ventricle injection of lipopolysaccharide, transgenic mice whose neurones overexpressed PTGS2 and non-transgenic control mice showed similar levels of inflammation, suggesting that PTGS2 from neurones does not play a role in neuroinflammation caused by the acute activation of the brain's innate immune response[61]. The effect of the conditional knockout of hippocampal microglial PTGS2 on POCD requires further investigation.

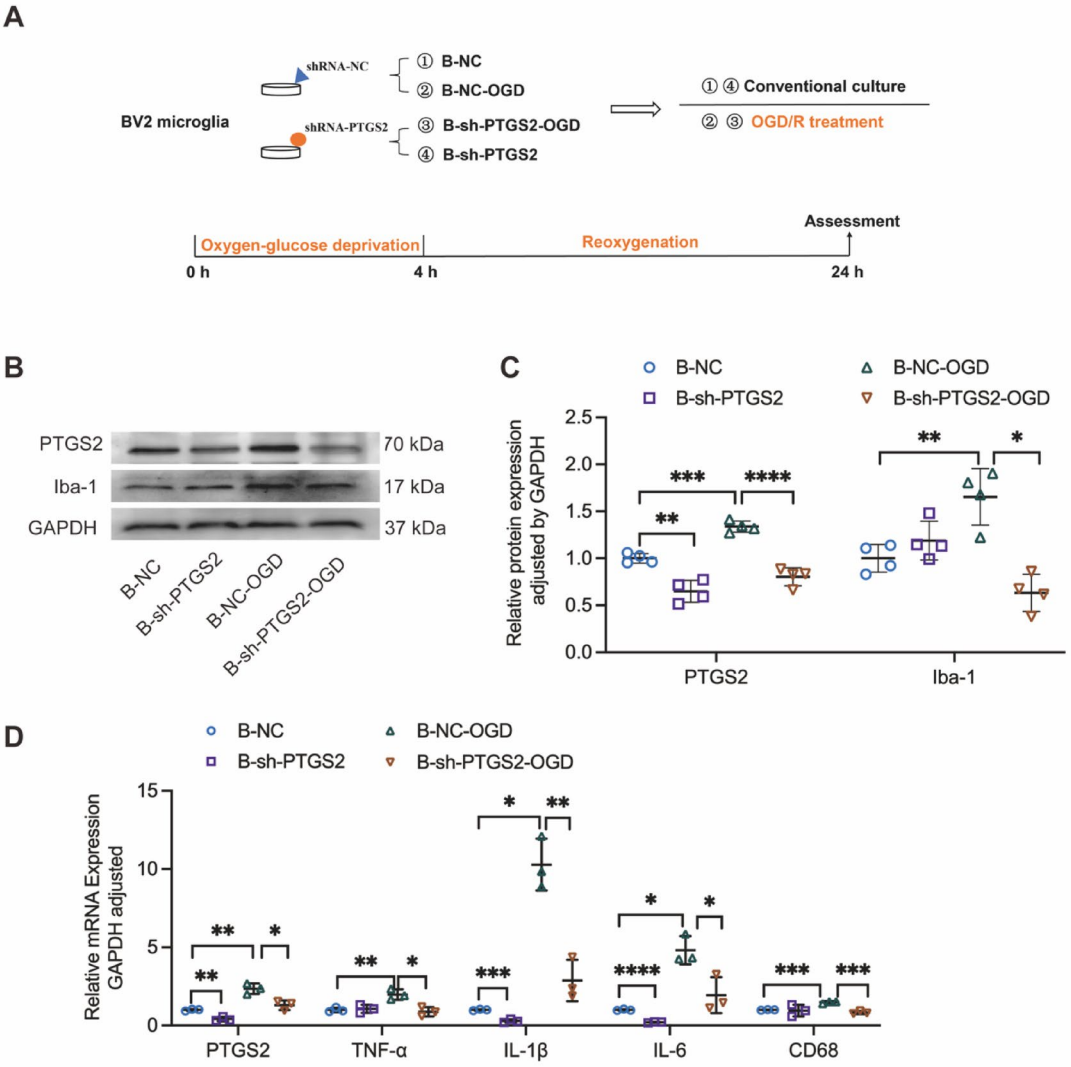

Fig. 6. PTGS2 are Required for OGD/R-induced Microglial Activation.

This study has some limitations. First, the sample was collected only after three days of modelling; therefore, more time points should be set for sample collection to understand the dynamic changes of relevant indicators during the development of POCD. Second, because in vitro experiments cannot fully reflect the in vivo state, the conclusions of the in vitro experiments need to be further verified by in vivo experiments. For example, an adeno-associated virus with a microglia-specific promoter was injected into the mouse hippocampus to obtain mice with low PTGS2 expression in hippocampal microglia.

Conclusion

In conclusion, this study demonstrates that PTGS2 is involved in the development of POCD and that its inhibition can effectively improve POCD. The underlying mechanism may be that targeting PTGS2 alleviates microglial activation, reduces the inflammatory response, and improves neuronal survival.

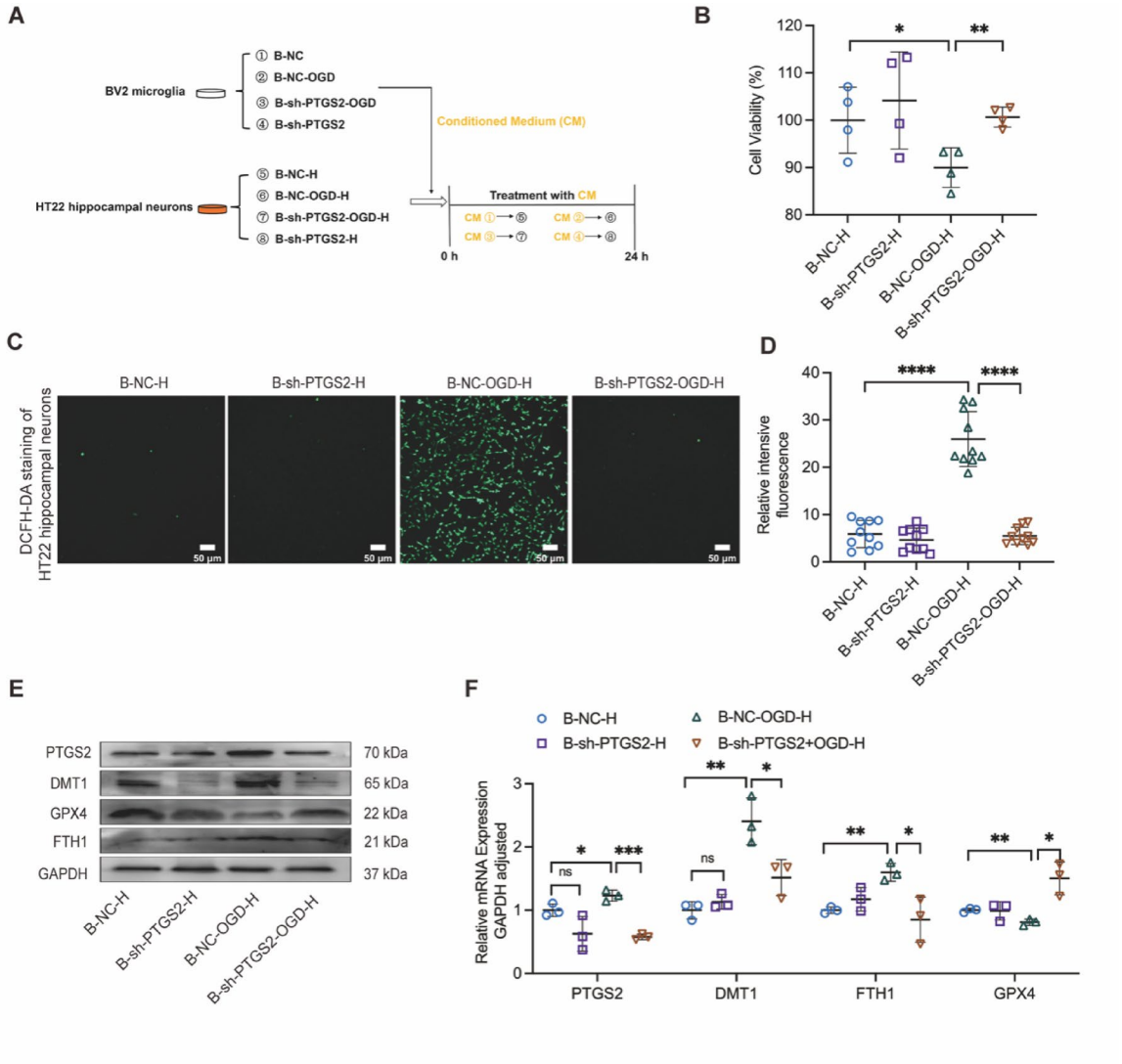

Fig. 7. PTGS2 Mediates OGD/R-induced Microglia Neurotoxicity.

Data availability

Data will be made available upon reasonable request from the corresponding author. RNA sequences of mice hippocampus were deposited in the National Center for Biotechnology Information (NCBI) repository. The BioProject accession number is PRJNA1175023 and the SRA records can be accessible with the following link: https://www.ncbi.nlm.nih.gov/bioproject/PRJNA1175023.

Received: 7 October 2024; Accepted: 5 May 2025
Published online: 19 May 2025

References

1. Monk, T. et al. Predictors of cognitive dysfunction after major noncardiac surgery. *Anesthesiology* **108**, 18–30. https://doi.org/10.1097/01.anes.0000296071.19434.1e (2008).
2. Duan, X. et al. Serum glial cell line-derived neurotrophic factor levels and postoperative cognitive dysfunction after surgery for rheumatic heart disease. *J. Thorac. Cardiovasc. Surg.* **155**, 958–965e951. https://doi.org/10.1016/j.jtcvs.2017.07.073 (2018).
3. Borchers, F. et al. Methodology of measuring postoperative cognitive dysfunction: a systematic review. *Br. J. Anaesth.* **126**, 1119–1127. https://doi.org/10.1016/j.bja.2021.01.035 (2021).
4. Pedemonte, J. et al. Postoperative delirium mediates 180-day mortality in orthopaedic trauma patients. *Br. J. Anaesth.* **127**, 102–109. https://doi.org/10.1016/j.bja.2021.03.033 (2021).
5. Yangzi, Z. et al. Inflammation disrupts the brain network of executive function after cardiac surgery. *Ann. Surg.* **277** https://doi.org/10.1097/sla.0000000000005041 (2021).
6. Yan, Y. et al. Neuroinflammation-mediated mitochondrial dysregulation involved in postoperative cognitive dysfunction. *Free Radic Biol. Med.* **178** https://doi.org/10.1016/j.freeradbiomed.2021.12.004 (2021).
7. Jennifer, T. et al. Postoperative delirium and changes in the blood-brain barrier, neuroinflammation, and cerebrospinal fluid lactate: a prospective cohort study. *Br. J. Anaesth.* **129** https://doi.org/10.1016/j.bja.2022.01.005 (2022).

8. Ruonan, Z. et al. Ultrasound-Assisted H(2) transmitter enables Hydrogen-Gene therapy to prevent Anesthesia/Surgery-Induced cognitive impairment. *Adv. Sci. (Weinh)*. https://doi.org/10.1002/advs.202414397 (2025).
9. Lai, I. et al. Blocking Kv1.3 potassium channels prevents postoperative neuroinflammation and cognitive decline without impairing wound healing in mice. *Br. J. Anaesth.* **125**, 298–307. https://doi.org/10.1016/j.bja.2020.05.018 (2020).
10. Liu, X. et al. Role of p53 methylation in manganese-induced cyclooxygenase-2 expression in BV2 microglial cells. *Ecotoxicol. Environ. Saf.* **241**, 113824. https://doi.org/10.1016/j.ecoenv.2022.113824 (2022).
11. Wang, D., Cabalag, C., Clemons, N. & DuBois, R. Cyclooxygenases and prostaglandins in tumor immunology and microenvironment of Gastrointestinal Cancer. *Gastroenterology* **161**, 1813–1829. https://doi.org/10.1053/j.gastro.2021.09.059 (2021).
12. Roulis, M. et al. Paracrine orchestration of intestinal tumorigenesis by a mesenchymal niche. *Nature* **580**, 524–529. https://doi.org/10.1038/s41586-020-2166-3 (2020).
13. Long, X. et al. Eosinophils protect against acetaminophen-induced liver injury through cyclooxygenase-mediated IL-4/IL-13 production. *Hepatology* **77** https://doi.org/10.1002/hep.32609 (2022).
14. Zhang, W. et al. Tumor homing chimeric peptide rhomboids to improve photodynamic performance by inhibiting Therapy-Upregulated Cyclooxygenase-2. *Small (Weinheim Der Bergstrasse Germany)*. **20**, e2309882. https://doi.org/10.1002/smll.202309882 (2024).
15. Stavros, M. et al. Risk factors for postoperative delirium in patients undergoing lower extremity joint arthroplasty: a retrospective population-based cohort study. *Reg. Anesth. Pain Med*. https://doi.org/10.1136/rapm-2019-100700 (2019).
16. Zeng, D. et al. Effect of parecoxib on postoperative delirium in patients with hyperlipidemia: a randomized, double-blind, single-center, superiority trial. *Int. J. Surg.* https://doi.org/10.1097/js9.0000000000002286 (2025).
17. Vizcaychipi, M. et al. The therapeutic potential of Atorvastatin in a mouse model of postoperative cognitive decline. *Ann. Surg.* **259**, 1235–1244. https://doi.org/10.1097/sla.0000000000000257 (2014).
18. Wang, Y. et al. MiR-214-3p prevents the development of perioperative neurocognitive disorders in elderly rats. *Curr. Med. Sci.* **42**, 871–884. https://doi.org/10.1007/s11596-022-2572-x (2022).
19. J, S. & Y-B, W., Z, C., J, L. & Parecoxib improves the cognitive function of POCD rats via attenuating COX-2. *Eur. Rev. Med. Pharmacol. Sci.* **23** https://doi.org/10.26355/eurrev_201906_18088 (2019).
20. Lang, H. et al. Small extracellular vesicles secreted by induced pluripotent stem cell-derived mesenchymal stem cells improve postoperative cognitive dysfunction in mice with diabetes. *Neural Regeneration Res.* **18**, 609–617. https://doi.org/10.4103/1673-5374.350205 (2023).
21. Fanning, J., Huth, S., Robba, C., Grieve, S. & Highton, D. Advances in neuroimaging and monitoring to defend cerebral perfusion in noncardiac surgery. *Anesthesiology* **136**, 1015–1038. https://doi.org/10.1097/aln.0000000000004205 (2022).
22. Poon, Y. et al. Disproportional cardiovascular depressive effects of isoflurane: serendipitous findings from a comprehensive re-visit in mice. *Lab Anim.* **50**, 26–31. https://doi.org/10.1038/s41684-020-00684-w (2021).
23. Zhao, Q. et al. Prenatal disruption of blood-brain barrier formation via cyclooxygenase activation leads to lifelong brain inflammation. *Proc. Natl. Acad. Sci. U. S. A.* 119, e2113310119 (2022). https://doi.org/10.1073/pnas.2113310119
24. Jin, X. et al. Baicalin mitigates cognitive impairment and protects neurons from microglia-mediated neuroinflammation via suppressing NLRP3 inflammasomes and TLR4/NF-κB signaling pathway. *CNS Neurosci. Ther.* **25**, 575–590. https://doi.org/10.1111/cns.13086 (2019).
25. Li, S. et al. Dental pulp stem cell-derived exosomes alleviate cerebral ischaemia-reperfusion injury through suppressing inflammatory response. *Cell Prolif.* **e13093** https://doi.org/10.1111/cpr.13093 (2021).
26. Steven Leary, W. U., Anthony, R., Cartner, S., Grandin, T. & Greenacre, C. Sharon Gwaltney-Brant, Mary Ann McCrackin, Robert Meyer, David Miller, Jan Shearer, Tracy Turner, Roy Yanong. AVMA Guidelines for the Euthanasia of Animals: (2020). (2020) Edition.
27. Kanehisa, M., Furumichi, M., Sato, Y., Matsuura, Y. & Ishiguro-Watanabe, M. KEGG: biological systems database as a model of the real world. *Nucleic Acids Res.* **53**, D672–D677. https://doi.org/10.1093/nar/gkae909 (2025).
28. Kanehisa, M. & Goto, S. KEGG: Kyoto encyclopedia of genes and genomes. *Nucleic Acids Res.* **28**, 27–30. https://doi.org/10.1093/nar/28.1.27 (2000).
29. Kanehisa, M. Toward Understanding the origin and evolution of cellular organisms. *Protein Science: Publication Protein Soc.* **28**, 1947–1951. https://doi.org/10.1002/pro.3715 (2019).
30. Vorhees, C. & Williams, M. Morris water maze: procedures for assessing Spatial and related forms of learning and memory. *Nat. Protoc.* **1**, 848–858. https://doi.org/10.1038/nprot.2006.116 (2006).
31. Liu, D. et al. BDE-47 induced PC-12 cell differentiation via TrkA downstream pathways and caused the loss of hippocampal neurons in BALB/c mice. *J. Hazard. Mater.* **422**, 126850. https://doi.org/10.1016/j.jhazmat.2021.126850 (2022).
32. Sun, J. et al. Ligustilide enhances hippocampal neural stem cells activation to restore cognitive function in the context of postoperative cognitive dysfunction. *Eur. J. Neurosci.* **54**, 5000–5015. https://doi.org/10.1111/ejn.15363 (2021).
33. Mehta, V., Johnston, A., Cheung, R., Bello, A. & Langford, R. M. Intravenous parecoxib rapidly leads to COX-2 inhibitory concentration of valdecoxib in the central nervous system. *Clin. Pharmacol. Ther.* **83**, 430–435. https://doi.org/10.1038/sj.clpt.6100304 (2008).
34. Evered, L. et al. Recommendations for the nomenclature of cognitive change associated with anaesthesia and surgery-2018. *Br. J. Anaesth.* **121**, 1005–1012. https://doi.org/10.1016/j.bja.2017.11.087 (2018).
35. Kunicki, Z. et al. Six-Year cognitive trajectory in older adults following major surgery and delirium. *JAMA Intern. Med.* **183**, 442–450. https://doi.org/10.1001/jamainternmed.2023.0144 (2023).
36. J, S. et al. Postoperative delirium in elderly patients is associated with subsequent cognitive impairment. *Br. J. Anaesth.* **119** https://doi.org/10.1093/bja/aex130 (2017).
37. Barber, P. et al. Cerebral ischemic lesions on diffusion-weighted imaging are associated with neurocognitive decline after cardiac surgery. *Stroke* **39**, 1427–1433. https://doi.org/10.1161/strokeaha.107.502989 (2008).
38. Zhang, F. et al. The immunometabolite S-2-hydroxyglutarate exacerbates perioperative ischemic brain injury and cognitive dysfunction by enhancing CD8 T lymphocyte-mediated neurotoxicity. *J. Neuroinflammation*. **19**, 176. https://doi.org/10.1186/s12974-022-02537-4 (2022).
39. Feng, L. et al. Association between cerebrovascular disease and perioperative neurocognitive disorders: a retrospective cohort study. *Int. J. Surg.* https://doi.org/10.1097/js9.0000000000000842 (2023).
40. Investigators, N. Perioperative Covert stroke in patients undergoing non-cardiac surgery (NeuroVISION): a prospective cohort study. *Lancet* **394**, 1022–1029. https://doi.org/10.1016/s0140-6736(19)31795-7 (2019).
41. Lan, F. et al. Diagnostic value of serum PTGS2 level for cognitive dysfunction in elderly patients undergoing hip arthroplasty. *Chongqing Yi Xue*, 1–14 (2022).
42. Perosa, V. et al. Hippocampal vascular reserve associated with cognitive performance and hippocampal volume. *Brain: J. Neurol.* **143**, 622–634. https://doi.org/10.1093/brain/awz383 (2020).
43. Santos-Pata, D. et al. Epistemic autonomy: Self-supervised learning in the mammalian Hippocampus. *Trends Cogn. Sci.* **25**, 582–595. https://doi.org/10.1016/j.tics.2021.03.016 (2021).
44. Dembo, G., Park, S. & Kharasch, E. Central nervous system concentrations of cyclooxygenase-2 inhibitors in humans. *Anesthesiology* **102**, 409–415. https://doi.org/10.1097/00000542-200502000-00026 (2005).

45. Mian, P., Yan-Lin, W., Fei-Fei, W., Chang, C. & Cheng-Yao, W. The cyclooxygenase-2 inhibitor parecoxib inhibits surgery-induced Proinflammatory cytokine expression in the hippocampus in aged rats. *J. Surg. Res.* **178** https://doi.org/10.1016/j.jss.2012.08.030 (2012).
46. Parkhurst, C. et al. Microglia promote learning-dependent synapse formation through brain-derived neurotrophic factor. *Cell* **155**, 1596–1609. https://doi.org/10.1016/j.cell.2013.11.030 (2013).
47. Basilico, B. et al. Microglia control glutamatergic synapses in the adult mouse hippocampus. *Glia* **70**, 173–195. https://doi.org/10.1002/glia.24101 (2022).
48. Xu, F. et al. Prolonged anesthesia induces neuroinflammation and complement-mediated microglial synaptic elimination involved in neurocognitive dysfunction and anxiety-like behaviors. *BMC Med.* **21**, 7. https://doi.org/10.1186/s12916-022-02705-6 (2023).
49. Debbie, A. E., Corbert, H., Karianne, G. E., Jörg, G. S., Inge, H. & H. & Staining of HLA-DR, Iba1 and CD68 in human microglia reveals partially overlapping expression depending on cellular morphology and pathology. *J. Neuroimmunol.* 309. https://doi.org/10.1016/j.jneuroim.2017.04.007 (2017).
50. D, I., Y, F. & K, T., S, S., T, D. & Enhanced expression of Iba1, ionized calcium-binding adapter molecule 1, after transient focal cerebral ischemia in rat brain. *Stroke* **32** https://doi.org/10.1161/01.str.32.5.1208 (2001).
51. Lin, W. et al. Role of calcium signaling Pathway-Related gene regulatory networks in ischemic stroke based on multiple WGCNA and Single-Cell analysis. *Oxidative Med. Cell. Longev.* **2021** (8060477). https://doi.org/10.1155/2021/8060477 (2021).
52. Tomimoto, H., Akiguchi, I., Wakita, H., Lin, J. & Budka, H. Cyclooxygenase-2 is induced in microglia during chronic cerebral ischemia in humans. *Acta Neuropathol.* **99**, 26–30. https://doi.org/10.1007/pl00007402 (2000).
53. Angela, R. Meloxicam improves object recognition memory and modulates glial activation after splenectomy in mice. *Eur. J. Anaesthesiol.* **29** https://doi.org/10.1097/EJA.0b013e3283534f56 (2012).
54. Li, S. et al. Dental pulp stem cell-derived exosomes alleviate cerebral ischaemia-reperfusion injury through suppressing inflammatory response. *Cell. Prolif.* **54**, e13093. https://doi.org/10.1111/cpr.13093 (2021).
55. Qian, Z. et al. Lipopolysaccharides upregulate Hepcidin in neuron via microglia and the IL-6/STAT3 signaling pathway. *Mol. Neurobiol.* **50**, 811–820. https://doi.org/10.1007/s12035-014-8671-3 (2014).
56. Pandur, E. et al. Fractalkine induces Hepcidin expression of BV-2 microglia and causes Iron accumulation in SH-SY5Y cells. *Cell. Mol. Neurobiol.* **39**, 985–1001. https://doi.org/10.1007/s10571-019-00694-4 (2019).
57. Galaris, D., Barbouti, A. & Pantopoulos, K. Iron homeostasis and oxidative stress: an intimate relationship. *Biochim. Et Biophys. Acta Mol. Cell. Res.* **1866**, 118535. https://doi.org/10.1016/j.bbamcr.2019.118535 (2019).
58. Zhong, H. et al. S-ketamine exposure in early postnatal period induces social deficit mediated by excessive microglial synaptic pruning. *Mol. Psychiatry*. https://doi.org/10.1038/s41380-025-02949-7 (2025).
59. Seta, F. et al. Renal and cardiovascular characterization of COX-2 knockdown mice. *Am. J. Physiol. Regul. Integr. Comp. Physiol.* **296**, R1751–1760. https://doi.org/10.1152/ajpregu.90985.2008 (2009).
60. Wan, Q. et al. Congestive heart failure in COX2 deficient rats. *Sci. China Life Sci.* **64**, 1068–1076. https://doi.org/10.1007/s11427-020-1792-5 (2021).
61. Aid, S., Parikh, N., Palumbo, S. & Bosetti, F. Neuronal overexpression of cyclooxygenase-2 does not alter the neuroinflammatory response during brain innate immune activation. *Neurosci. Lett.* **478**, 113–118. https://doi.org/10.1016/j.neulet.2010.04.076 (2010).

Acknowledgements

The authors thank Jianguo Feng and Jing Jia for their help of experimentation.

Author contributions

Xuelian Li: Methodology, Formal analysis, Investigation, Data curation, Writing – original draft, Writing – review & editing, Visualization. Xuemei Li: Methodology, Formal analysis, Investigation. Qixin Zhang: Software, Data curation. Yiyun Li: Investigation, Supervision. Yingshun Zhou: Conceptualization, Methodology, Investigation, Resources, Writing – review & editing, Supervision. Jun Zhou: Conceptualization, Methodology, Investigation, Resources, Writing – review & editing, Supervision. Xiaoxia Duan: Conceptualization, Methodology, Formal analysis, Investigation, Resources, Data curation, Writing – review & editing, Visualization, Supervision, Project administration, Funding acquisition.

Funding

This work was supported by the Campus-institute strategic cooperation projects(2024SNXNYD01);the Science and Technology Department of Luzhou (grant number 2023 JYJ001).

Declarations

Competing interests

The authors declare no competing interests.

Ethical approval

This study was reviewed and approved by the Ethics Committee of Laboratory Animal Care and Welfare of Southwest Medical University with the approval number [SWMU20220029].

Additional information

Supplementary Information The online version contains supplementary material available at https://doi.org/10.1038/s41598-025-01121-z.

Correspondence and requests for materials should be addressed to Y.Z., J.Z. or X.D.